



# MEASUREMENT OF MOLTEN POOL TEMPERATURE FIELD IN TWIN-ROLL CASTING OF THIN STRIP STEEL

H. Zhang\*, X.G. Li †, W.Z. Zhao †

\*College of Information Science and Engineering, Northeastern University, Shenyang, 110819, Liaoning, China.  
 E-mail address: zhanghua@mail.neu.edu.cn

*This is an open access article distributed under the Creative Commons Attribution License, which permits unrestricted use, distribution, and reproduction in any medium, provided the original work is properly cited*

## ARTICLE DETAILS

## ABSTRACT

### Article History:

Received 02 october 2017  
 Accepted 06 october 2017  
 Available online 11 october 2017

### Keywords:

Temperature field Measurement;  
 Molten Pool; Twin-roll casting;  
 Finite element analysis; heat transfer.

To measure the temperature distribution of molten pool in twin-roll strip casting, a new method based on the soft measurement of temperature field and on-line measurement of fixed point temperature was presented. A three-dimensional model on coupled turbulent flow and heat transfer, was firstly established. With regard of the four outlets nozzle, the numerical solution of temperature field was achieved and compared with the real time measurement in order to calibrate the model. A function library, thus, is derived and characterized by the relationship between temperature distribution and main features such as the submerged depth of delivery system, casting temperature, contacting arc, roll speed, casting angel, material properties and roll gap. By applying real time adjustment to the function library, this new method may increase the accuracy, reliability and rapidness of the measurement of molten pool temperature field.

## 1. INTRODUCTION

Compared with conventional strip casting, the twin-roll strip casting is regarded as the most prospective technology of near-net-shape casting [1,2]. Such process may reduce energy consumption and production costs, may improve production efficiency and product quality [3,4]. Besides, twin-roll strip casting is a very complicated process, in which turbulent flow, heat transfer, and solidification, plastic deformation can be completed in less than one second. Temperature has great influence on the quality and mechanical properties of strips so that the rationality and uniformity of temperature distribution in molten pool is of primary importance in twin-roll strip casting. As it is unable to measure all the distribution by experiment during such a short time, up to the present, almost all research efforts have been concentrated to study temperature simulation calculations [5,6].

C.A. Santos, et al. [7] and Q. Li, et al. [8] studied the effects of the casting parameters on the temperature, but their researches ignored the nozzles and the differences along the axial direction. B. Wang [9,10] developed the water modeling and simulated the twin-roll strip casting, but the rotation of the casting rollers was not be considered. Since 2000, the study of coupled thermal-flow equations and simulation model has been proposed [11-14]. W. S. Kim et al. [11] discussed a beneficial impact of submerged nozzle on the stabilization of the free-surface zone. W.M. Wang et al. [12] stimulated the coupled temperature and flow by finite element, but the heat transfer along the contact surface was considered linear. Y. Fang, et al. [13] studied the temperature field of stainless steel by experiment and a finite element (FE) model, and give the relationship between the roll gaps or roll radius and the position of the freezing point. J.H. Dong [14] developed a novel-type delivery system consisting of a special feeding device and delivery device in order to obtain the uniformity of temperature distribution. However, nearly all the research did not adopt four outlets, which can receive a much more stable temperature field.

In this study, three dimensional theoretical equations and simulation models were established for the coupled turbulent flow, heat transfer and solidification. The coefficient of heat transfer between molten metal

and rolls, influence of the rollers' rotation, latent heat and the four outlets are all taken into consideration. Compared to the real time measurement temperature, the model was calibrated. Based on this model, a function library on temperature distribution was founded in terms of major features.

## 2. Mathematical model

In a twin-roll strip casting, the liquid steel is fed through a delivery system (nozzle) from a tundish into a wedge-shaped molten pool formed by the two-counter rotating water-cooled rolls and two side dams. In this case, steel can solidify in an extremely short time and is machined into strip steel at the exit, as shown in Figure 1. During this process, the turbulent fluid flow, heat transfer and solidification exist simultaneously.

### 2.1 Physical assumption

Considering the practical process of casting, the assumptions are as follows:

- (1)The heat caused by plastic deformation and friction is very little, which, compared to heat brought in by liquid steel, can be ignored.
- (2)The stress field is only related to temperature distribution, while the phase transformation and rolling force is ignored.
- (3)The turbulent effect is approximated by k-ε model.
- (4)The glide and segregation between the roller and the solidified strip is negligible.
- (5)The roller surface is perfectly clean and no plastic deformation occurs on the roller.

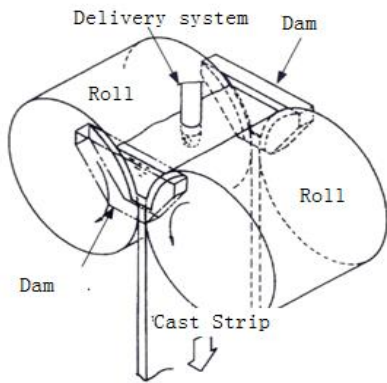


Figure 1. Schematic diagram of the twin-roll strip casting

(6) Material properties depend on temperature, while the physical parameters of the casting rollers are constant.

(7) The liquid steel is assumed as incompressible Newtonian fluid.

(8) The delivery system is located in the center of the molten pool. Therefore, the temperature distributions on both sides are equal, only 1/4 of the melting pool can be used.

## 2.2 Controlling equation

(9) Under the above assumption, the following transport equations including Continuity equation, Momentum equation (turbulent Navier-Stokes equation) and Energy equation were presented to describe the liquid metal forming behavior in the twin-roll strip casting.

(1) Continuity equation

$$\frac{\partial(u_x)}{\partial x} + \frac{\partial(u_y)}{\partial y} + \frac{\partial(u_z)}{\partial z} = 0 \quad (1)$$

Where  $u_x$ ,  $u_y$  and  $u_z$  are velocity components in the x, y, z directions.

(2) Momentum equation

$$\frac{\partial(\rho u_x u_x)}{\partial x} + \frac{\partial(\rho u_x u_y)}{\partial y} + \frac{\partial(\rho u_x u_z)}{\partial z} = \rho g_x - \frac{\partial P}{\partial x} + \frac{\partial}{\partial x} \left( \mu_{eff} \frac{\partial u_x}{\partial x} \right) + \frac{\partial}{\partial y} \left( \mu_{eff} \frac{\partial u_x}{\partial y} \right) + \frac{\partial}{\partial z} \left( \mu_{eff} \frac{\partial u_x}{\partial z} \right) + T_x \quad (2)$$

$$\frac{\partial(\rho u_y u_x)}{\partial x} + \frac{\partial(\rho u_y u_y)}{\partial y} + \frac{\partial(\rho u_y u_z)}{\partial z} = \rho g_y - \frac{\partial P}{\partial y} + \frac{\partial}{\partial x} \left( \mu_{eff} \frac{\partial u_y}{\partial x} \right) + \frac{\partial}{\partial y} \left( \mu_{eff} \frac{\partial u_y}{\partial y} \right) + \frac{\partial}{\partial z} \left( \mu_{eff} \frac{\partial u_y}{\partial z} \right) + T_y \quad (3)$$

$$\frac{\partial(\rho u_z u_x)}{\partial x} + \frac{\partial(\rho u_z u_y)}{\partial y} + \frac{\partial(\rho u_z u_z)}{\partial z} = \rho g_z - \frac{\partial P}{\partial z} + \frac{\partial}{\partial x} \left( \mu_{eff} \frac{\partial u_z}{\partial x} \right) + \frac{\partial}{\partial y} \left( \mu_{eff} \frac{\partial u_z}{\partial y} \right) + \frac{\partial}{\partial z} \left( \mu_{eff} \frac{\partial u_z}{\partial z} \right) + T_z \quad (4)$$

Where  $\rho$  is the density of the liquid steel,  $g_x$ ,  $g_y$  and  $g_z$  are components of gravity acceleration;  $\mu_{eff}$  is effective viscosity

coefficient.

(3) Energy equation

$$\frac{\partial}{\partial t} (\rho C_p T) + \frac{\partial}{\partial x} (\rho u_x C_p T) + \frac{\partial}{\partial y} (\rho u_y C_p T) + \frac{\partial}{\partial z} (\rho u_z C_p T) = \frac{\partial}{\partial x} \left( K_{eff} \frac{\partial T}{\partial x} \right) + \frac{\partial}{\partial y} \left( K_{eff} \frac{\partial T}{\partial y} \right) + \frac{\partial}{\partial z} \left( K_{eff} \frac{\partial T}{\partial z} \right) + Q_v \quad (5)$$

Where  $Q_v$  is heat source,  $K_{eff}$  is effective thermal conductivity.

## 2.3 Turbulent model

(1) Governing transport equations for turbulent kinetic energy  $k$

$$\frac{\partial(\rho u_x k)}{\partial x_i} + \frac{\partial(\rho u_y k)}{\partial x_j} + \frac{\partial(\rho u_z k)}{\partial x_k} = \frac{\partial}{\partial x_i} \left( \frac{\mu_t}{\sigma_k} \frac{\partial k}{\partial x_i} \right) + \frac{\partial}{\partial x_j} \left( \frac{\mu_t}{\sigma_k} \frac{\partial k}{\partial x_j} \right) + \frac{\partial}{\partial x_k} \left( \frac{\mu_t}{\sigma_k} \frac{\partial k}{\partial x_k} \right) + \mu_t \phi - \rho \varepsilon \quad (6)$$

(2) Dissipation rate of turbulent kinetic energy  $\varepsilon$

$$\frac{\partial(\rho u_x \varepsilon)}{\partial x} + \frac{\partial(\rho u_y \varepsilon)}{\partial y} + \frac{\partial(\rho u_z \varepsilon)}{\partial z} = \frac{\partial}{\partial x} \left( \frac{\mu_t}{\sigma_\varepsilon} \frac{\partial \varepsilon}{\partial x} \right) + \frac{\partial}{\partial y} \left( \frac{\mu_t}{\sigma_\varepsilon} \frac{\partial \varepsilon}{\partial y} \right) + \frac{\partial}{\partial z} \left( \frac{\mu_t}{\sigma_\varepsilon} \frac{\partial \varepsilon}{\partial z} \right) + C_1 \mu_t \frac{\varepsilon}{k} \phi - C_2 \rho \frac{\varepsilon}{k} \varepsilon \quad (7)$$

In addition, the internal energy is changed when the steel transfer from liquid into solid. Apparent Capacity Method was adopted to deal with this problem in which the solidification latent heat was replaced by apparent capacity.

## 2.4 Boundary condition

(1) At the entrance of liquid steel,  $T = T_0$ ,  $V_x = 0$ ,  $V_y = -V_{in} \sin \alpha$ ,  $V_z = -V_{in} \cos \alpha$ ,  $k = aV_{in}^2$ ,  $\varepsilon = k^{1.5} / R$ .

Where  $T_0$  is the entrance temperature,  $V_x$ ,  $V_y$  and  $V_z$  are velocity components in the x, y, z directions,  $V_{in}$ ,  $R$  and  $\alpha$  is the speed of the delivery system entrance, size of the entrance and outlet angle respectively.

(2) On the pool surface,  $-k \frac{\partial T}{\partial n} = \varepsilon \sigma (T^4 - T_a^4)$ ,  $V_y = 0$ ,

$\frac{\partial V_x}{\partial y} = 0$ ,  $\frac{\partial V_z}{\partial y} = 0$ ,  $\frac{\partial k}{\partial y} = 0$ ,  $\frac{\partial \varepsilon}{\partial y} = 0$ . Where  $\varepsilon$  and  $T_a$  is

emissivity of the liquid steel and the temperature of the air respectively.

(3) At the symmetry interface,  $Q = 0$ ,  $V_z = 0$ ,  $\frac{\partial V_x}{\partial z} = 0$ ,

$\frac{\partial V_y}{\partial z} = 0$ ,  $\frac{\partial k}{\partial z} = 0$ ,  $\frac{\partial \varepsilon}{\partial z} = 0$ .

(4) At the contact interface with roller,  $-k \frac{\partial T}{\partial n} = h_{cont} (T - T_R)$ ,

$V_x = V \sin \theta$ ,  $V_y = -V \cos \theta$ ,  $V_z = 0$ , Where  $h_{cont}$  and  $T_R$  is the equivalent heat transfer coefficient and the temperature of the roller respectively. The calculated models among the

coefficient, casting speed, and location between molten metal and rolls in different regions were given [15].

(5) At the contact interface with side dam,

$$-k \frac{\partial T}{\partial n} = h_m (T - T_b), V_z = 0.$$

## 3. Numerical simulation of temperature fields

In this study, the finite element method and ANSYS package were used for the discretization of the partial differential equation. The 304 stainless steel was selected as the casting

material and the simulation conditions are given in Table 1. The 1/4 model of the melting pool was established because of its symmetry, and was meshed into 300000 nodes due to the adoption of four outlets.

Table 1. Parameters of twin roll strip casting

Parameters	Value
Diameter of the roller [m]	0.5
Length of the roller [m]	0.254
Height of the molten pool [m]	0.105, 0.125 and 0.16
Thickness of the strip [m]	0.001, 0.002 and 0.003
Width of the strip [m]	0.200-0.254
Depth of the nozzle submerging [m]	0.01, 0.02, 0.03
Size of the nozzle [m]	0.016×0.008
Pour temperature [°C]	1490, 1510, 1530
Casting speed [m/s]	0.5, 0.6, 0.7
Contact angle [°]	35, 40, 45
Roller speed [r/min]	20

The two radiation thermometers were installed to measure the temperature of the pool surface and the exit of the steel strip. Through a series of corrections, the model was calibrated.

4. Result and Discussion

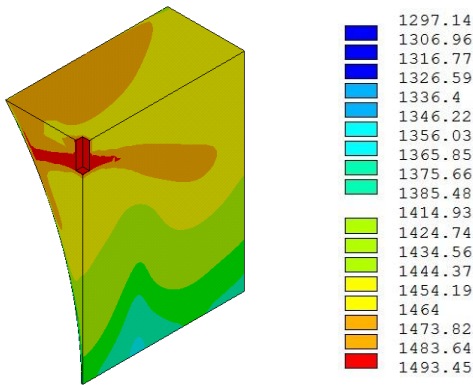
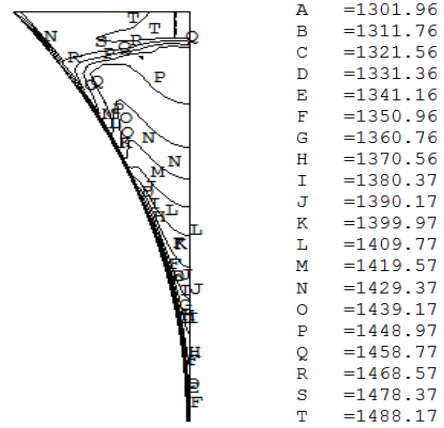


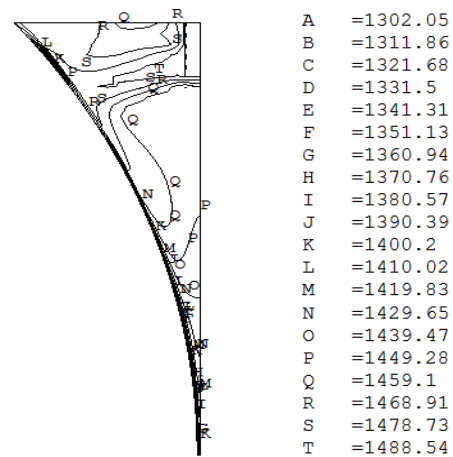
Figure 2. Temperature field distribution of the molten pool

Figure 2 gave the temperature field distribution of the molten pool. The simulated conditions are that the contact angle of molten pool and casting roller is 40 degree, nozzle's export angle is 20 degree, nozzle feeding depth is 20mm, the speed of casting roller is 20 r/m, and the casting temperature is 1490 °C. The temperature is more homogenized due to the adoption of four outlets which engender two vortices that work as stirrers. As a result, the calculated pool surface temperatures are in good agreement with the measured values.

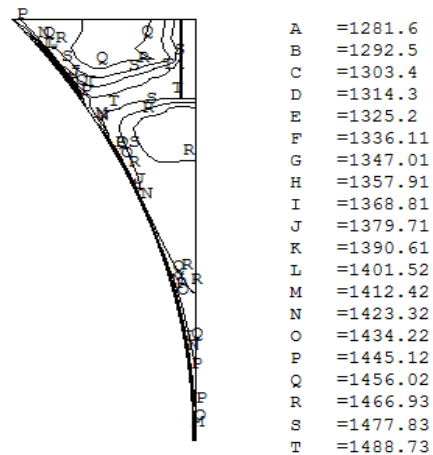
Figure 3 shows the temperature distribution of centrosymmetric area under different feeding depth. From the figure we can see that when the depth is 10mm, since the molten pool in this area is relatively large, the circulation caused by casting roll is not obvious, so that the temperature of middle area is low, with 47° C of deviation on the width. When the depth is 30mm, circulation caused by side dam fluid will enhance thus increasing the center area temperature, with a 70°C deviation on the width. We can see that now the distribution is more uneven.



(a) 10mm



(b) 20mm



(c) 30mm

Figure 3. Temperature field of centrosymmetric area under different submerged depth

In the same way, the relationships between the temperature distribution and other parameters were achieved. Based on analysis of the factors, seven major features-- nozzle feeding depth, casting temperature, contacting arc, roll speed, casting angel, material properties and roll gap are chosen and used to establish the function library. Since the library cannot traverse all situation, there shall be finely tuned according to the process conditions to make the measurement more efficient and more precise.

## 5. Conclusion

In accordance coupled the turbulent flow, heat transfer and solidification, the 3D theoretical equations and simulation model have been conducted. Four outlets are adopted as they can form vortices and stabilize the temperature. In consideration of heat transfer coefficient change with the roller speed and location, latent heat and the effect of rollers' rotation, the coupled temperature field of molten pool were simulated and the result is consistent with the measured one, which confirms the availability of this model. The function library, reflecting the relationship among the temperature distribution and main influence factors, concludes to improve the accuracy, reliability and rapidness of the measurement of molten pool temperature field.

## Acknowledgements

This study was supported by National Key Research Development Planning Project of China (2004CB619108).

## References

- [1] M. Yamada, K. Isogami, H. Hosoda, et al. "World's first commercial twin drum strip casting process at Hikari Works of Nippon Steel Corporation", *Steel world*, 7, pp. 49-54, (2002).
- [2] R. Wechsler. "The status of twin-roll casting technology", *Scandinavian Journal of Metallurgy*, 32(1), pp. 58-63,(2003).
- [3] L.W. Richard, J.F. John. "The castrip process for twin-roll casting of steel strip", *AISE Steel Technology*, 79(9), pp. 69-74, (2002).
- [4] Z. Nikolai. "Comparison of continuous strip casting with conventional technology", *ISIJ International*, 43(8), pp. 1115-1127, (2003).
- [5] C.M. Park, W.S. Kim, G.J. Park. "Thermal analysis of the roll in the strip casting process", *Mechanics Research Communication*, 30, pp. 297-310, (2003).
- [6] K. Hauser, K. Dittenberger, S. Hahn, et al. "Dynamic 3D heat transfer simulation of continuous casting", *International Journal of Cast Metals Research*, 22, pp. 115-118, (2009).
- [7] C.A, Santos, T.A. Spim Jr., A. Garcia. "Modeling of solidification in twin-roll strip casting", *Journal of Materials Processing Technology*, 102, pp. 33-39,(2000).
- [8] Q. Li, Y.K. Zhang, L.G. Liu, et al. "Effect of casting parameters on the freezing point position of the 304 stainless steel during twin-roll strip casting process by numerical simulation", *Journal of Mater Science*, 47, pp. 3953-3960, (2012).
- [9] B. Wang, J.Y. Zhang, J.F. Fan. "Water modeling of twin-roll strip casting", *Journal of Iron and Steel Research, International*, 13(1), pp. 14-17, (2006).
- [10] B. Wang, J.Y. Zhang, Y. Zhang. "Numerical and physical simulation of a twin-roll strip caster", *Journal of University of Science and Technology, Beijing*, 13(15), pp. 393-396, (2006).
- [11] W. S. Kim, D.S. Kim, A.V. "Kuznetsov. Simulation of coupled turbulent flow and heat transfer in the wedged-shaped pool of a twin-roll strip casting process", *International Journal of Heat and Mass Transfer*, 43, pp. 3811-3822, (2000).
- [12] W.M. Wang, J. Zhong, W.P. Yu, et al. "The finite element simulation of heat flow solidification in twin-roll strip casting", *Metallurgy engineering*, 27(2), pp.61-67, (2007).
- [13] Y. Fang, Z.M. Wang, Q.X. Yang, et al. "Numerical simulation of the temperature fields of stainless steel with different roller parameters during twin-roll strip casting", *International Journal of Minerals, Metallurgy and Materials*, 16(3), pp. 304-308, (2009).
- [14] J.H. Dong, M. Chen, N. Wang. "Characteristics of fluid flow and temperature field of twin-roll steel strip casting with a novel-type delivery system", *Journal of Iron and Steel Research, International*, 22(10), pp. 885-891,(2015).
- [15] G.M. Cao, C.G. Li, Z.Y. Liu, et al. "Numerical simulation of molten pool and control strategy of kiss point in a twin-roll strip casting process", *Acta Metallurgica Sinica*, 12(6), pp. 459-468, (2008).

